Uhley HN (1961) Study of the transmembrane action potential, electrogram, electrocardiogram and vectorcardiogram of rats with left ventricular hypertrophy. Am J Cardiol **7:** 211–217
Wendt-Gallitelli MF, Ebrecht G, Jacob R (1979) Morphological alterations and their functional interpretation in the hypertrophied myocardium of Goldblatt hypertensive rats. J Mol Cell Cardiol **11:** 275–287
Wolinsky H (1971) Effects of hypertension and its reversal on the thoracic aorta of male and female rats. Morphological and chemical studies. Circ Res **28:** 622–637

Computer Simulation of Arrhythmias in a Network of Coupled Excitable Elements

FRANS J.L. VAN CAPELLE AND DIRK DURRER

SUMMARY **Arrhythmias were simulated in sheets or cables, consisting of coupled excitable elements, which were characterized by a simple regenerative mechanism. The geometry of the network, the amount of coupling among individual elements, and the properties of the elements relating to excitability, automaticity, and duration of the refractory period could be adjusted arbitrarily in an interactive computer program. When a critical amount of coupling was present between automatic and nonautomatic cells, sustained repetitive activity could be initiated and stopped by stimulation of the elements. Using this mechanism, it also was possible to evoke reciprocal activity in a one-dimensional cable. In uniform sheets of coupled elements, circus movement of the activation front could be evoked. The presence of an obstacle or dispersion of the refractory periods of the elements was not a prerequisite for the initiation of circus movements. The vortex of circus movements in the homogeneous sheets consisted of elements which were inactivated by depolarizing currents from the circulating wavefront. In sheets of sufficient size, multiple vortices could be present.** ***Circ Res 47: 454–466, 1980***

WE used computer simulation to study the possible role of spatial interaction among excitable elements in the mechanisms underlying cardiac arrhythmias, of both the focal and the reentrant type. Intuitively, the mechanism of focal tachycardias is thought to reside mainly in the ionic properties of the cell membrane, whereas the involvement of many interacting cells is a prerequisite for reentrant arrhythmias. We were interested in whether it would be possible to evoke both focal and reentrant arrhythmias in a synthetic sheet consisting of a primitive kind of excitable element, and whether the influence the elements exert on each other would play an important role in the genesis and maintenance of these arrhythmias. As it turns out, many of the features of clinical and experimental tachycardias could be simulated rather easily in such a model, and the results suggest that the role of spatial interaction among cardiac cells may be of considerable importance in both types of arrhythmia.

Although many model studies of impulse propagation have been published, relatively few of them deal with sheets consisting of large numbers of elements. Notable exceptions are an early compu study (Moe et al., 1964), demonstrating the imp tance of dispersion of the duration of the refract periods of the elements in the mechanism of fib lation, and an elegant hybrid study (Gul'ko a Petrov, 1972) on circus movement of the activat front in homogeneous sheets. The reason for t scantiness is that long trains of action potenti have to be calculated for many elements simu neously in this type of study, and this requires enormous amount of computation, even on a la computer. We dealt with this problem using a s plified model for the individual excitable eleme and interactive computer techniques. With the h of interactive computer programs, irrelevant s tions may be skipped and interesting episodes n be repeated immediately, using other parame settings, or displaying the signals of different ments. The simulation is performed very muc in an actual experiment. For instance, before set the stimulus strength, one has to determine sti lus threshold levels, to set the stimulus sequen and to make decisions about the location of stimuli. The computer dialogue is formulated in e usual electrophysiological terminology. In acco dance with this practice, electrophysiological ter s such as tachycardia, refractory period, etc., will e applied freely in the present text. Although it m seem inappropriate to refer to a computer as having a tachycardia, we believe that the practical advan-

From the Department of Cardiology and Clinical Physiology, University Hospital Wilhelmina Gasthuis, Amsterdam, The Netherlands, and the Interuniversity Cardiological Institute, The Netherlands.
Address for reprints: F.J.L. van Capelle, Department of Clinical Physiology, Wilhelmina Gasthuis, Eerste Helmersstraat 104, 1054 EG Amsterdam, The Netherlands.
Received October 18, 1979; accepted for publication April 24, 1980.

tages of discussion in these terms largely outweigh such objections.

The present study centered on two issues. The first was to determine whether a triggerable focal tachycardia (that is, a focus which can be turned on and off by a single stimulus) can be evoked in a system of coupled elements, and, if so, to investigate whether its mechanism would be a likely one from an electrophysiological point of view. The second aim was to see whether an obstacle would be a prerequisite for circus movement tachycardia (CMT) to occur in a simulation, and if not, to investigate the nature of the vortex or center of such a tachycardia. Both phenomena, triggerable focal activity and CMT without the presence of an obstacle, were easy to evoke, and the present paper deals with the mechanisms involved.

Methods

The model consists of up to 650 excitable elements, arranged in a geometry which is to be specified at the start and which may be changed during execution of the simulation. As an example, a square lattice geometry is illustrated in Figure 1. The elements are coupled through passive resistances, which may be set individually to arbitrary values (although no more than five different values are accepted by the program). The elements need not be all identical. Elements may be deleted or changed at any time during the simulation, and coupling resistances may be deleted, changed, or added between any two elements. The network of resistors overlying the elements in Figure 1 may be thought of as representing the intracellular space. The lower side of the elements is connected to the extracellular space, which is assumed to be at zero potential at all times.

From the instantaneous transmembrane potentials of the elements and from the values of the coupling resistance, the currents through the intracellular maze are known. Thus the currents emerging from the elements at the nodes of the network can be calculated. Subtraction of the ionic currents flowing through the same elements at that point in time then yields the capacitive current flowing through that particular element. In this way the rate of rise of the action potentials of the elements can be calculated, and integration of this quantity yields the time course of the transmembrane voltage of all elements.

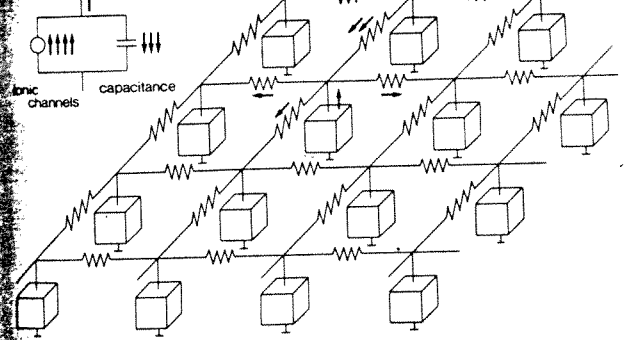

FIGURE 1 *Example of arrangement of excitable elements. The bottom side of the individual elements (extracellular space) is always at zero potential. The top side is connected by a resistive network, which represents the intracellular space. The current emerging from an element consists of an ionic and a capacitive component (inset). This current matches the sum of the currents flowing to the element through the intracellular space.*

Before starting a simulation, it is necessary to define the types of elements to be used. In our simulation, this was done by specification of two membrane voltage-current relations, a steady state inactivation function, and a few parameters. An adequate choice of these quantities would result in elements possessing the desired electrophysiological characteristics. A separate interactive program which displays the relevant functions and parameters, together with the resultant action potentials and voltage clamp currents, facilitates adjustment of the properties of the elements. In this way, a library of excitable elements was created from which a selection could be made when a simulation was performed.

Next, the arrangement of the elements must be specified. After specification of the dimensions of the sheet, the graphic terminal will initially display a square lattice containing the elements. Now, pointing at the elements with a joystick, individual cells may be deleted, leaving a "hole" in the sheet. In the same way, existing cell connections may be deleted, and new ones installed, resulting in a network of arbitrary complexity. Using the same technique, the cell type of individual elements and the resistance of individual cell connections may be changed. Since it is confusing to display more than about 10 traces simultaneously on the terminal, a selection of elements to be monitored on the terminal is made. This is equivalent to the procedure of positioning of the recording electrodes in an actual experiment. In the same way, the stimulating sites are selected with the joystick.

After specification of the stimulus sequence, the simulation can be started. While the simulation progresses, the action potentials of the selected elements are displayed on the graphic terminal and stored on a disk. Whenever an element is activated, the activation time also is written on a separate disk file, yielding a complete survey of the activation sequence.

The Model

In the present membrane model, only two variables of state, the transmembrane voltage V and a generalized excitability parameter Y, are retained. Y can have any value between 0 (maximal excitability) and 1 (complete inexcitability). The state of an element is at any time completely determined

by its V and Y values. Thus a single parameter Y plays here a role similar to that of m, n, and h in the classical Hodgkin-Huxley kinetics. The behavior of V and Y is described by the following first-order differential equations:

$$C\dot{V} = -Yi_1(V) - (1 - Y)i_0(V) + i_{ex} \quad (1a)$$

$$T\dot{Y} = Y_{inf}(V) - Y. \quad (1b)$$

The first of these equations describes the current balance of the elements. It states that the capacitive membrane current CV must be supplied by an ionic transmembrane current, determined by V and Y, and an external current i_{ex}. This external current may enter the cell from neighboring elements, or be injected by an intracellular microelectrode. The ionic current is a weighted average between the two currents, i_1 (V) and i_0 (V), both of which are independent of Y. Y appears only as a weighting factor. i_0 (V) is the current-voltage relation when the membrane is maximally excitable (Y = 0). It must display a region of negative resistance to make the regenerative excitation process work. i_1 (V), on the other hand, is the current-voltage relation for a completely inexcitable membrane. The functions i_0 (V) and i_1 (V) have to be supplied to the computer program before the simulation starts. They determine, to a large extent, what the characteristics of the element under consideration will be.

Equation 1b supplies the rate of change of excitability as a function of V and Y. When V is kept constant (as in a voltage clamp experiment), Y will move exponentially toward the final value, Y_{inf} (V). The function Y_{inf} (V) must also by supplied to the computer program. It must be an S-shaped function, increasing from zero when V is more negative than the resting potential to 1 at more positive values of the membrane potential.

Once the functions i_0 (V), i_1 (V), and Y_{inf} (V) have been specified, only the values of the membrane capacitance C and the time constant T of the activation/inactivation process have to be supplied to specify completely the characteristics of the element. C and T are constants, independent of V. To make the computations as quickly as possible, the functions must have a simple form. For Y_{inf} (V) and i_1 (V), piecewise linear functions consisting of three or four segments were taken. Instead of i_0 (V), the function f (V) = i_0 (V) − i_1 (V) was stored, since this resulted in a somewhat more efficient version of the algorithm. The function f (V) consisted of three sections: the first and last ones were straight lines and the middle one was cubic, fitted in such a way that both the function f and its derivative df/dV were continuous.

The functions i_0 (V), i_1 (V) and Y_{inf} (V) must be selected with some care. For instance, if more than one singular point occurs in the Y-V plane (the phase plane), failure to repolarize may result. The duration of the action potential is determined largely by the value of i_1 (V) at the plateau level of the action potential and the upstroke velocity, the maximum value of the inward current i_0 (V). To create elements with the desired electrophysiological properties and an attractive shape of the action potential, a separate interactive program was written. After specification or on-line modification of i_0, i_1, and Y_{inf}, together with C and T, this program plots the resulting action potentials on the graphic screen as a function of time and as a trajectory in the phase plane, as explained below. Furthermore, it asks the operator what voltage clamp steps to apply, including preconditioning steps if desired, and plots the resulting tracing also on the graphic screen. Using this information, the operator may adapt the functions or the parameters and try in this way to optimize the element with respect to the properties desired in that particular instance. By means of the hard copy facilities, documentation of suitable elements was stored. The use of the phase plane representation was essential in the

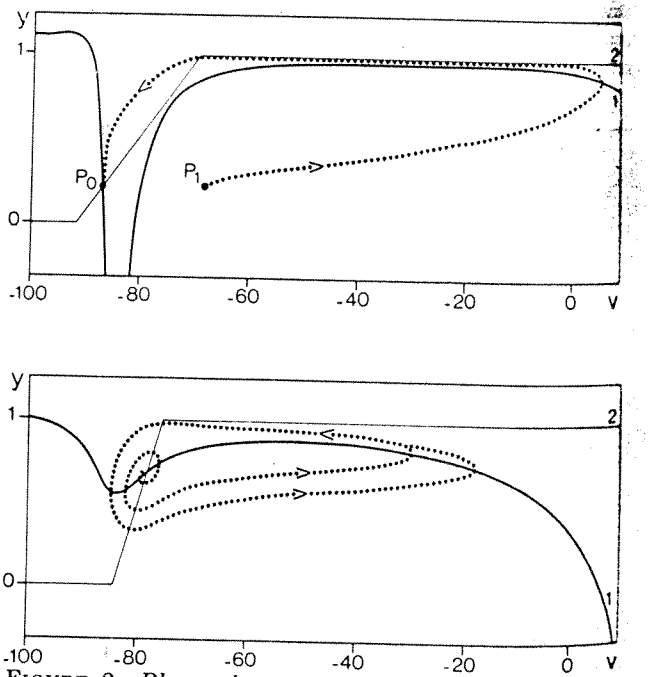

FIGURE 2 *Phase plane representation of action potentials for a non-pacemaker (upper panel) and a pacemaker element (lower panel). Abscissa is membrane potential; ordinate is the excitability parameter. Dotted line is trajectory of an action potential; heavy line, labeled "1," is locus where direction of trajectory is vertical; thin line, labeled "2," is locus where trajectories run horizontally. Upper panel: the phase point of a non-automatic element is instantaneously depolarized and displaced from the resting point P_0 to P_1. The phase point moves along the indicated trajectory to return to the resting position after repolarization. Lower panel: The phase point of a pacemaker element is positioned initially close to the resting point. It spirals outward until a steady trajectory is reached. This corresponds to subthreshold oscillations developing into a sustained rhythmic activity of full-blown action potentials.*

construction of satisfactory elements.

Phase Plane Representation

In this model, the state of any element is determined completely by the parameters V and Y. The properties of the elements can be visualized conveniently by the use of the so-called phase plane representation. The phase plane is the V-Y plane, and an action potential can be represented as a trajectory in this plane An example is given in Figure 2. The resting state of the element is represented by point P_0. Here the membrane potential is negative, and the excitability is high, since Y is close to zero. Stimulation of the element with a very short current pulse will not change the excitability instantaneously. However, the membrane potential is instantaneously displaced to a value that is determined by the amount of charge delivered to the membrane capacitance. On stimulation, the phase point thus jumps immediately to point P_1. From here, the phase point starts to move spontaneously along the trajectory indicated. It is assumed that the element is not coupled to other cells, so that $i_{ex} = 0$ in equation 1a. From point P_1, the phase point moves rapidly in a horizontal way. This part of the trajectory corresponds to the upstroke of the action potential. The depolarization of the membrane causes inactivation to take place, resulting in an increase of Y. For this reason the trajectory turns upward. It is clear that during repolarization the same range of membrane voltages must be transversed in the opposite direction. This happens, of course, at higher values of Y, since the excitability is then abolished. A gradual return toward point P_0 completes the loop.

This last part of the trajectory is of importance for the electrophysiological properties of the element. If the phase point descends vertically toward the resting point P_0, the resting membrane voltage is restored much earlier than the excitability. In this case, the refractory period of the element tends to outlast the action potential duration. This property is valuable if one considers mimicking atrioventricular (AV) node cells. A horizontal return to the resting point, on the other hand, represents the situation in which excitability is completely restored before the action potential has completely repolarized. A depolarization that is smaller than the diastolic threshold intensity now is sufficient to activate the element, and a phase of superexcitability results.

The shape of the trajectory in the phase plane, and therefore also the shape of the corresponding action potential, is determined to a large extent by two functions, the vertical and horizontal isoclines, which may be plotted in the phase plane. Assuming no coupling (i.e., $i_{ex} = 0$) and setting $C\dot{V} = 0$ in equation 1a, we obtain from the righthand part, $Y = i_0/(i_0 - i_1)$. This function represents the locus of points in the phase plane, where no trajectory can have a horizontal component, so that all trajectories must intersect this function in a vertical direction. In the same way, the function $Y = Y_{inf}(V)$ can only be intersected horizontally by any trajectory. These two functions are plotted on the graphic terminal as soon as the voltage current relations are entered and are very useful in the interactive process of adjusting the voltage-current relations in order to obtain a particular kind of action potential.

The resting point is, of course, defined by the intersection of those two functions, since at this point no spontaneous movement of the phase point occurs. It does not follow, however, that the resting point so defined must be stable. Three situations of interest are here. The resting point may be unconditionally stable and nonperiodic. Trajectories will approach the resting point in the manner shown in the upper panel of Figure 2. The resting point also may have a periodic character. In this case, the trajectories will approach P_0 in a spiral fashion. This results in damped oscillations in the time course of the action potentials at the end of the repolarization phase. If the resting point is unstable, the trajectories will not approach the resting point but will encircle it instead. We can, however, start a trajectory from the resting point, which will escape, spiralling outward and resulting in an incrementing oscillation that eventually reaches threshold, giving rise to an action potential. During subsequent cycles, the phase point loops around the point P_0, the trajectory converging rapidly toward a so-called stable limit cycle. Elements of this kind are eligible as pacemaker cells in our study. It is possible to choose the parameters in such a way that these pacemakers exhibit many familiar electrophysiological properties. For instance, the pacemaker elements used in this study can be slowed down and stopped by the application of hyperpolarization current. It is equally possible to construct nonautomatic cells, which can be turned into pacemakers by depolarizing current.

From Equation 1, other important electrophysiological properties of the elements may be derived. During a voltage clamp situation, the lefthand part of Equation 1a is kept zero. This is achieved by supplying just the right amount of clamp current, i_{ex}. The clamp current, needed to maintain the voltage at its prescribed value, may thus be derived from the righthand part of Equation 1a: $i_{ex} = Yi_1 + (1 - Y)i_0$. Y is not constant, but approaches its final value $Y_{inf}(V_0)$ exponentially. The time course of i_{ex} can thus be plotted, with Equation 1b, and is also a valuable aid in the construction and selection of elements.

The simulation program was written in FORTRAN and executed on a PDP11/34 computer with 32 k memory under the RT 11 single-job monitor. A simple Euler method was used for the integration of the equations, and solutions were checked occasionally by repetition of a simulation with smaller time steps. The display of the simulated action potentials and the interactive dialogue during exe-

cution of the program was done on a Tektronix 4012 graphic terminal and, during the latter stages of this study, on a Megatek 7000 graphic system. Hard copies of the results were plotted, if desired, on a VERSATEC electrostatic printer/plotter. Activation times of the individual elements were stored on a disk file which could be used subsequently to construct isochronal maps of the activation sequence.

Results

Focal Tachycardias

Figure 3 demonstrates the effect of tightness of cell coupling on the shape of the action potentials and on the rhythm in a simulation consisting of two nonidentical pacemaker elements. When coupling was absent (R = infinite), the elements fired at different rates, and they could also be distinguished easily by the shapes of their action potentials. In the case of weak coupling (R = 100), each element influenced the other's rate of firing, resulting in a slight arrhythmia. Entrainment may occur under these circumstances, as was the case when R = 100, where an exact 4:3 ratio existed between the frequencies of the elements. It can be seen that the depolarization rate of the upper element was influenced by the lower cell. When the coupling was tight enough (R = 20), the cells beat synchronously and at the same frequency, but differences in shape of the action potentials still persisted. These disappeared with further reduction of the coupling resistance (R = 0.5). In that stage, it was no longer possible to identify the separate elements on the basis of their rate or the shape of their action potentials.

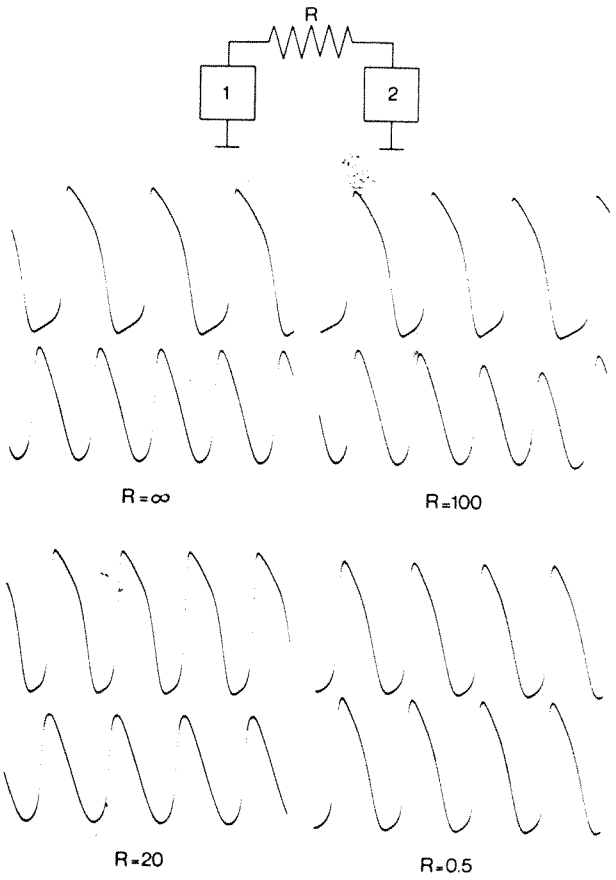

FIGURE 3 *Influence of coupling resistance (R) on action potential configuration of two different pacemaker elements. At R = infinity, the intrinsic rates and shapes of both elements are clearly different. At R = 100, the rates are different, but a 4:3 synchronization is present. At R = 20, the faster element leads, and the shapes of the action potentials are still different. At R = 0.5, the elements fire simultaneously), and can no longer be distinguished by their shapes.*

In Figure 4 the interaction of a pacemaker (PM) and a non-pacemaker (NP) element is demonstrated. The resting potential of the uncoupled NP element was about the same as the most negative potential occurring in the PM element during diastolic depolarization. When there was no coupling (Fig. 4A), the NP element was completely silent and the PM fired at its intrinsic rate. When the coupling was weak (Fig. 4B), subthreshold responses were visible in the NP cell; these grew in amplitude as the the coupling became tighter, until the NP cell became activated (Fig. 4C). The action potential of the NP cell then had a pronounced foot, corresponding to the latency caused by the slow charging of the membrane of the NP cell. Inversely, the delayed action potential of the NP cell was reflected as a slight prolongation of the duration of the action potential of the PM element. When the coupling resistance was reduced further, the latency disappeared and the action potentials became increasingly similar. Ultimately the elements could no longer be distinguished on the basis of the configuration of the respective action potentials (Fig. 4E). The frequency was somewhat lower than the intrinsic rate of the pacemaker (Fig. 4A). This was due to a reduction of the slope of diastolic depolarization, which was caused by the hyperpolarizing current flowing from the NP cell to the PM element during the latter part of phase 4.

These effects depend, of course, on the relative sizes of the elements. In the model, it is easy to reduce the size of an element; one simply has to reduce all the transmembrane currents and the membrane capacitance proportionally, leaving the other parameters unchanged. The PM element in Figure 5 was identical to the one shown in Figure 4, except for a 5-fold reduction in cell size. The intrinsic action potential was identical in shape to the element in Figure 4A but it can be seen that the reduction of the firing frequency, when coupling was installed, was much more prominent (Fig. 4, B-D). Also, the reflection of the delayed action potentials of Figure 5C on the PM cell was then clearly visible as a distinct hump. When the coupling was very tight, the repetitive activity of the PM cell was

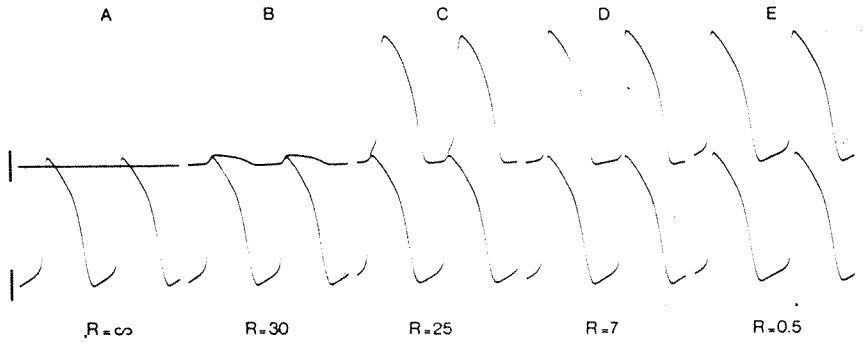

F RE 4 *Effects of decrease of the coupling resistance between a pacemaker (lower trace) and a non-pacemaker (u er trace) element. Vertical bars indicate identical membrane voltage range for both elements. A: Upper element is ent; B: local responses are present in upper trace; C: a foot precedes the activation of the upper element; D: a c in amount of phase 4 depolarization becomes apparent in the upper trace; E: action potentials of both elements a dentical. Note the lengthening of the interval as coupling becomes tighter.*

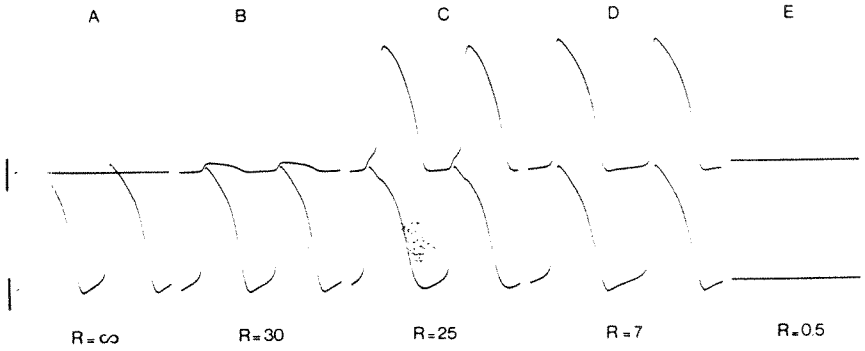

FIGURE 5 *Same as Figure 4, after reduction in size of the pacemaker element. The influence of the non-pacemaker element on the rate is much more pronounced, and at tight coupling the system is no longer spontaneously active.*

inhibited completely (Fig. 5E). This does not imply that the elements were not excitable: both elements could be successfully stimulated. This is demonstrated in the left panel on Figure 6 when the coupling resistance was just low enough to ensure that the elements did not start repetitive activity spontaneously. A single stimulus in the NP element not only evoked an action potential in both elements, but also acted as the start of sustained rhythmic activity. A clue to the mechanism of this phenomenon follows from the right panel of Figure 6, where the coupling resistance was somewhat lower. In this case, the action potential evoked by the stimulus was followed by oscillatory activity, which in the present case faded out. If the first oscillatory response after the action potential had reached threshold, as in the left panel, a sustained tachycardia would have resulted.

The same mechanism may be implemented easily in simulations containing more elements. To exclude all possibility of circus movements, the phenomenon is demonstrated on a linear cable geometry, consisting of 40 elements (Fig. 7). All elements were identical non-automatic cells except elements 37, 38, and 39 in the tail end of the cable, which were pacemaker cells. However, the cell coupling was so tight that the spontaneous activity of the pacemaker elements was suppressed by the non-pacemaker neighbor cells. On stimulation of element 1, activation propagated through the cable

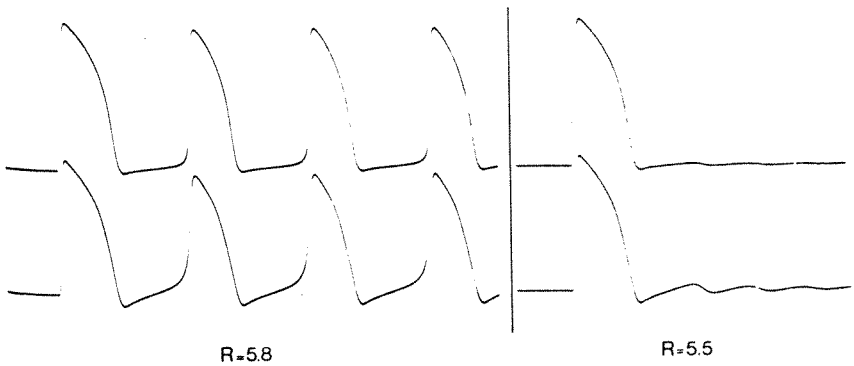

FIGURE 6 *The same configuration as in Figure 5, at critical values of the coupling resistance. The system is initially stable and silent, but stimulation of the upper element starts a sustained rhythmic activity (left panel). If the value of the coupling resistance is somewhat smaller, the stimulated response is followed by damped subthreshold oscillations (right panel).*

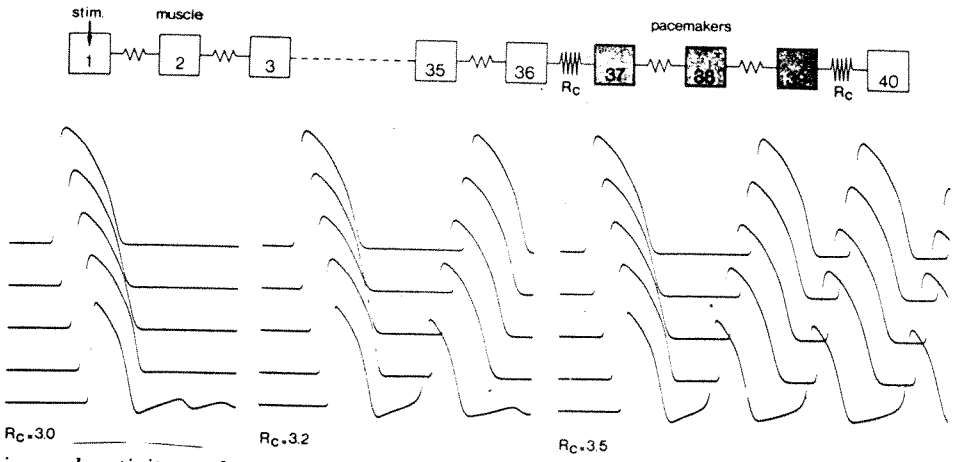

FIGURE 7 *Reciprocal activity and onset of tachycardia in a cable, consisting of 37 non-pacemaker elements and three pacemaker elements. The value of the coupling resistance Rc between the pacemaker region and the other elements is varied. Stimulation is performed at the first element at the left, and recording sites are along the cable, the lowest trace representing one of the pacemakers in the tail of the cable. The system is initially stable. Propagated activity along the cable is followed by subthreshold oscillations in the tail when Rc equals 3.0. At somewhat larger values of Rc, a single reciprocal activation or sustained rhythmic activity of the pacemaker region is evoked.*

and reached the pacemakers in the tail. In the left panel, the coupling resistance was too low (R = 3) to permit sustained pacemaker activity. However, damped subthreshold oscillations can be seen in the pacemaker cells. In the right panel, the coupling resistance was higher (R = 3.5), resulting in the onset of sustained rhythmic activity, which was conducted retrogradely along the cable. An interesting intermediate case is presented in the middle panel, where the coupling resistance was just critical (R = 3.2). In this case, there was just one extra activation in the pacemaker cells, which was conducted retrogradely along the cable. It can be seen that this second activation of the pacemaker elements was of a poor quality with regard to action potential amplitude and rate of rise. It is for this reason that the subthreshold oscillation at the end of the second action potential did not result in further full-blown activations.

The question now arises whether the sustained activity, started in Figure 7, also may be turned off again by a single stimulus. Properly timed stimulation of the tail end of the cable may indeed turn off the tachycardia. The time interval in which a stimulus on element 40 was effective in stopping the tachycardia was however quite small. Stimulation of element 1 was not effective in stopping the tachycardia, since the retrogradely conducted activity protected the focus in the tail end of the cable from antegrade activity. On the other hand, properly timed repetitive stimulation of element 1 did result in termination of the tachycardia.

Circus Movement Tachycardias

Circus movement tachycardia also could be induced in a sheet of sufficient size. Figure 8 demonstrates how a circus movement tachycardia could be set up. A square sheet was defined, having edges consisting of 23 elements. Then a hole was created in the sheet, by elimination of all center elements, leaving a ring, consisting of the outer elements, which was three elements wide. A stimulus applied at stimulus site 1 (left panel) resulted in two activation fronts along both sides of the ring, which collided at the opposite corner of the sheet. A second stimulus, having a strength of 3× diastolic threshold, was applied at site 2 at the shortest coupling interval which would result in propagated activity at all. Under these conditions, the antegrade wavefront was blocked close to its origin, whereas the retrograde wavefront was conducted backward and subsequently started a circus movement tachycardia. The time interval within which stimulation of site 2 would result in initiation of a tachycardia is illustrated in the tracings of Figure 8 by a small horizontal bar. Once initiated, the tachycardia could be stopped in essentially the same way: stimulation of a point along the circuit at the appropriate time resulted in a wavefront traveling in the opposite direction, which would abolish the circulating wavefront by a collision at the other side of the sheet. This simulation is, of course, quite similar to Mines' (1914) classical experiments, in which the conditions for circus movement of excitation in heart muscle were defined initially.

It has been confirmed experimentally that no hole or other obstacle need be present for circus movement tachycardias to occur. Allessie et al. (1973, 1976, 1977) demonstrated similar tachycardias in the isolated left atrium of the rabbit heart. The vortex of the tachycardia consisted of normally excitable fibers which were more or less inactivated during the tachycardia, but showed perfectly normal action potentials during regular stimulation of the preparation. Moreover, the authors showed, by

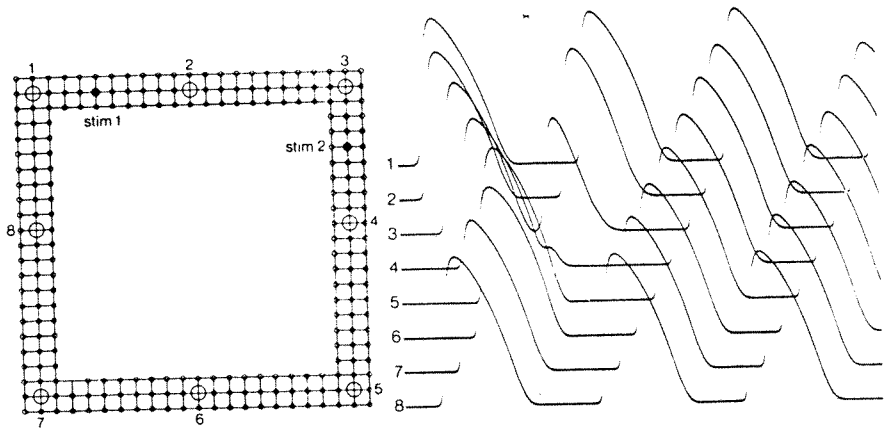

FIGURE 8 *Initiation of a circus movement tachycardia in a ring of non-pacemaker elements. Positions of stimulation (black circles) and recording (unfilled circles) are shown in the diagram. Stimulation of site 1 results in two wavefronts, which collide at the opposite side of the ring. Stimulation of site 2 during the interval indicated by the small bar above the tracings, results in retrograde propagation of the premature impulse, which is blocked in antegrade direction (note the local response in trace 4).*

careful mapping, that the vortex of the steady state tachycardia does not always coincide with the site of which the first return pathway was localized.

A similar kind of tachycardia could be evoked in a two-dimensional sheet of coupled elements. In a uniform sheet, consisting of identical elements coupled by identical resistances, where no dispersion in refractory period or other cell properties existed, circus movement tachycardias could be initiated in several ways. The easiest method was to make an L-shaped cut in the sheet, starting from the middle of the upper edge, and to stimulate at the top left side of the "L," forcing the wavefront to circle around the cut. It was sometimes necessary to stimulate at a high frequency, resulting in a shortening of the duration of the action potentials and in decrement of the conduction velocity. If the cut then was repaired and stimulation stopped at the moment that a wavefront arrived at the right side of the cut, a continuous circus movement could be set up. As a second method to introduce a circus movement in a homogeneous sheet, a special stimulation sequence was used. The position of eight stimulus sites and the nine recording sites in a 15 × 15 element grid is shown in Figure 9. To initiate a circus movement tachycardia, a plane wavefront was first set up through the sheet by quasi-simultaneous stimulation of electrodes A to E. The resultant wavefronts merged into a single plane wave, which traversed the sheet. This is illustrated in the first cycle of the tracings of Figure 9, where elements 1, 2, and 3 were activated simultaneously, followed by the middle row (elements 4, 8, and 9) and, finally, by the lower elements 5, 6, and 7.

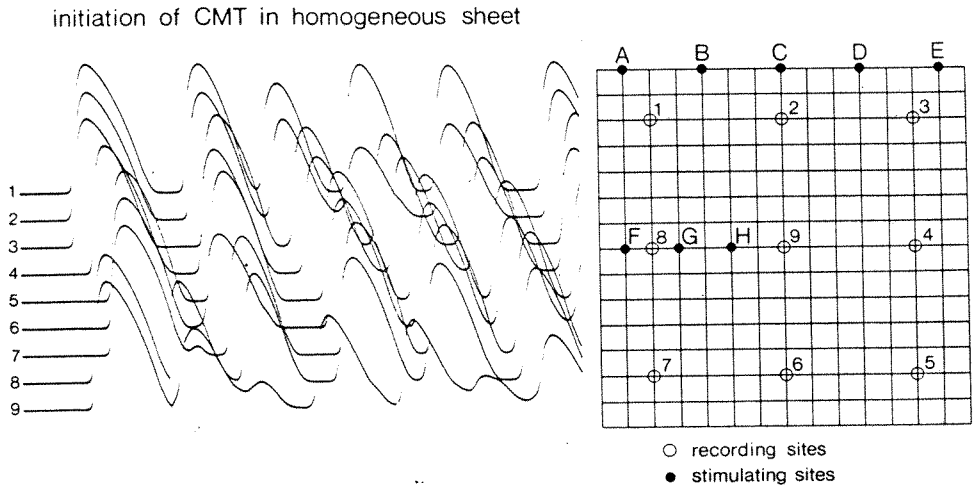

FIGURE 9 *Initiation of circus movement tachycardia in a homogeneous sheet. Filled circles are stimulus sites; unfilled circles correspond to tracings. A stimulus is applied within a short time interval to the five stimulation sites, A–E, located at the upper edge of the sheet. Stimulation of the other three stimulus sites (F, G, and H) at the appropriate time results in the onset of a circus movement tachycardia.*

Thereafter, at a certain critical coupling interval, a second stimulus was applied simultaneously to stimulating sites F, G, and H. The resulting activation was blocked antegradely, close to the stimulus sites (note the local response in element 7). The retrograde wavefront did propagate, invading the upper part of the sheet (element 1), turning right and downward at the opposite side of the sheet (elements 2, 3, 4, etc.). Depending on the coupling interval, a short run of two or three activations or a sustained tachycardia would occur.

The depression of the activity and the irregularity of element 9 is noteworthy. The reason for this behavior becomes clear if we consider Figure 10. The activation sequence of the elements is plotted in this figure in the form of isochronal lines. The first panel shows the planar wave front traversing the sheet and the second panel shows the pathway of the extrasystolic beat, which was blocked antegradely and traveled a circular route. As activation time, we took the moment a fixed potential level was reached by the action potential. This fixed level was at about 40% of the amplitude of normal action potentials. Consequently, local responses were not measured. The "holes" in the isochronal maps represent regions where no action potentials of sufficient magnitude were present during the interval depicted in the map. Thus, the first action potential

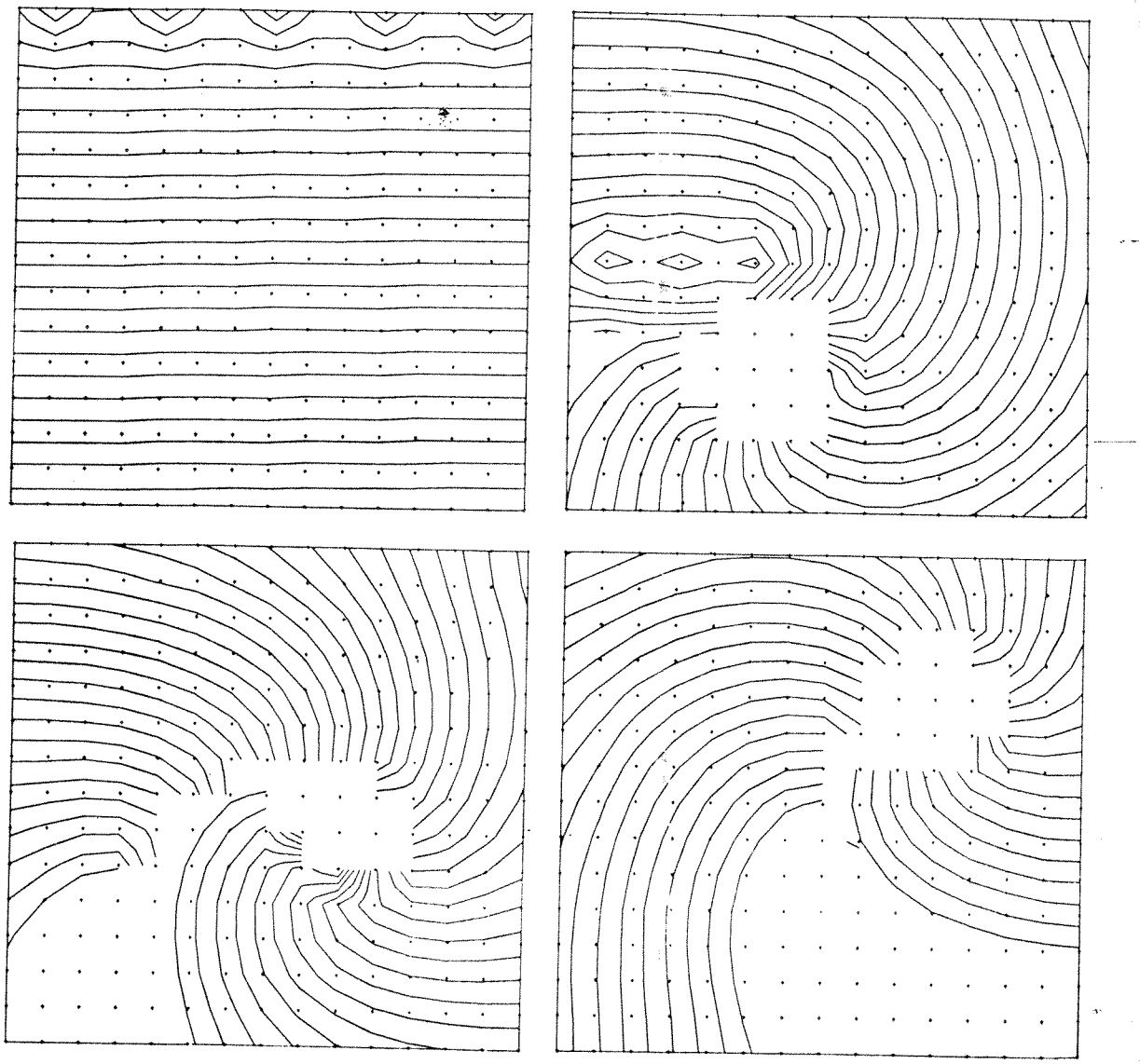

FIGURE 10 *Isochronal lines corresponding to the initiation of the tachycardia shown in Figure 9. The distance between the lines corresponds to 20 time steps. Left upper panel: plane wave caused by the conditioning stimulus. Right upper panel: the premature beat, which is blocked in the antegrade direction, starts a clockwise circus movement. The last isochronal line of this panel corresponds to the first one of the left lower panel. The right lower panel is a continuation of the left lower panel.*

of element 9 in Figure 9 corresponds to the planar wave of the first panel of Figure 10; the second, depressed action potential corresponds to the extrasystole whose path is shown in the second panel of Figure 10. The local response corresponds to the second passage of the wavefront from left to right through the upper part of the sheet (third panel), and the next action potential corresponds to the wavefront which travels ¾ cycle later upward through the left half of the sheet. It can be seen that (1) the vortex of the circus movement was not fixed, but could move through the sheet, and (2) elements belonging to the vortex did not repolarize properly because of the depolarizing current flowing toward them from the activated cells in the immediate vicinity. The tachycardia in Figure 10 did not stop spontaneously before the end of the simulation, which was about 50 cycles later. The vortex did not stabilize in a certain position, but kept moving over the sheet. As a result, the slight irregularity of the rhythm, apparent in Figure 9, persisted.

The susceptibility of a sheet for circus movement tachycardias depends on several factors, the most important ones being the size of the sheet and the refractory period of the elements. The larger the sheet, the easier to evoke CMT's. The effective size of a sheet depends on the number of elements, but also on the coupling among them. It is useful to express the size of the sheet in terms of length constants of a cable, consisting of the same elements and coupling resistances as used in the sheet. The sheet of Figure 9, which was very loosely coupled, was about 30 space constants long along the edges. Using the same elements as in Figure 9, we reduced the effective size of the sheet either by reduction of the number of elements (leaving the coupling resistances unchanged) or by reduction of the coupling resistances (leaving the number of elements constant). In either case, the critical effective size of the sheet for sustained circus movements to occur was about 20 length constant along the edges of the sheet. In smaller sheets only runs of 2–12 cycles were observed.

We compared the characteristics of CMT's in a homogenous sheet with progressively smaller holes in the middle of the sheet. We found that (1) if the hole was large, the frequency was determined by the time required for the wavefront to circle around the hole, as is to be expected. Changes in coupling resistance affected the frequency accordingly, since the conduction velocity is proportionate to the square root of the coupling resistance. (2) If the hole was small or absent, the frequency was determined mainly by the refractory period of the elements, and little affected by changes in coupling resistance. (3) Suppression of the tachycardia by regular stimulation at twice diastolic threshold intensity was easy when a large hole was present. In contrast, stimulation of the homogenous sheet would have an effect only if the stimulus site happened to be in or close to the vortex. In that case, however, the only effect generally was an immediate shift of the vortex to another position in the sheet, without termination of the tachycardia.

The question arises as to whether more complex forms of arrhythmias can occur also. Figure 11 shows an instance in which three separate vortices were present. To initiate this tachycardia, several cuts were made and repaired at the appropriate moments. The 3-fold circus movement persisted for

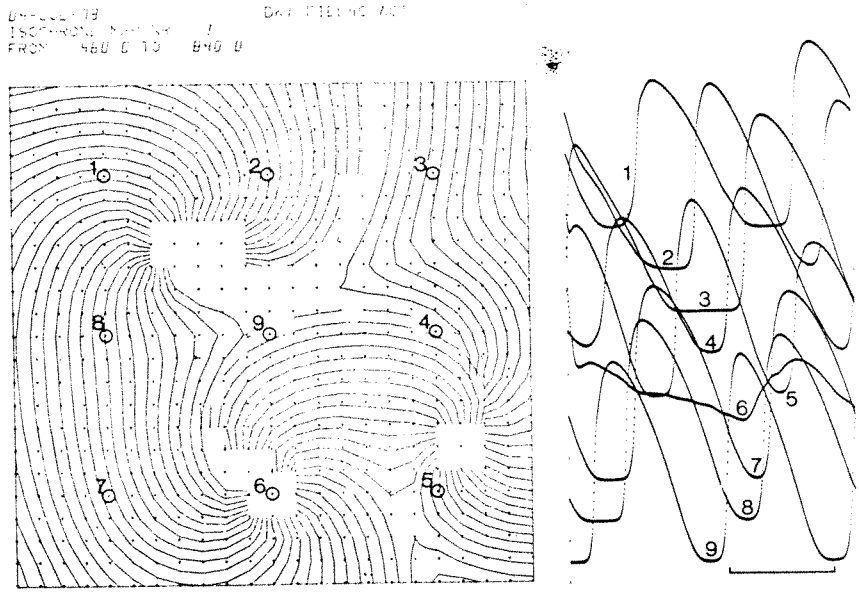

FIGURE 11 *Complex arrhythmias, consisting of three circus movements. The horizontal bar under the tracings corresponds to the interval depicted in the isochrone map. Tracings correspond to positions indicated by unfilled circles.*

a couple of beats, whereafter one wavefront was blocked near the edge of the sheet. The other vortices remained active during the rest of the stimulation.

Discussion

In principle, the mechanism of arrhythmias in a synthetic excitable network can be investigated and understood completely. This asset is offset by fundamental and practical limitations. The fundamental question is that of how representative the model is for cardiac tissue. This restricts the use of simulation to the heuristics. The presence of certain phenomena in a simulation merely indicates that the corresponding mechanism cannot be excluded a priori in cardiac tissue. This may lead subsequently to new experiments, or to rescrutiny of earlier experimental findings.

The practical limitations in the present simulation study are not to be underestimated. In the first place, the number of elements must not be too small for a simulation to be realistic. The space constant of cardiac tissue is in the order of 1 mm. In the sheets used in the present study, the distance between two elements varied from 1 to 2 space constants. The sheets therefore correspond with pieces of cardiac tissue of about 2–3 cm. To do justice to the functional syncytial nature of the myocardium, it would be preferable to use still more elements. Unfortunately, the amount of computer time required for such very large simulations would at present be prohibitive on our minicomputer.

Furthermore, the electrical behavior of the membranes has to be specified for each of the elements used. Several complete and sophisticated mathematical descriptions, based on Hodgkin-Huxley kinetics, do exist (McAllister et al., 1975; Beeler and Reuter, 1977). The problem here is 2-fold. Arrhythmias tend to occur in the slowly conducting tissues, such as the AV node, and more importantly in ischemic myocardial tissue. The ionic descriptions, on the other hand, tend to concentrate on healthy ungulate Purkinje tissue or ventricular myocardium. It therefore seems less reasonable to use these models in studies of arrhythmia. In the second place, the equations to be used in our simulations must be solved individually for every element. Thus the speed of the solution will be inversely proportional to the number of excitable elements used. In arrhythmia studies, we usually need a train of many action potentials in every episode, making the simulation extremely time consuming. Therefore it becomes necessary to reduce the ionic equations to the simplest form which permits us to retain basic physiological properties such as excitation, repolarization, refractoriness, possibility of phase 4 depolarization and pacemaker activity, and dependence of the upstroke velocity on the membrane potential. This meant that, in practice, we had to restrict ourselves to elements with a low upstroke velocity, which are more representative of nodal or depressed myocardial cells than of healthy myocardium in Purkinje fibers.

It is remarkable how well very simple models do perform in this respect. For this reason they have been used extensively in the past. Van der Pol (and van der Mark) (1926, 1928) were the first to apply the relaxation oscillator, a member of this class of models, to the heart beat (especially to AV conduction). Starting from the familiar equations for the harmonic oscillator, he made the damping dependent on the instantaneous amplitude of the oscillator. As a result, the waveform became more or less a square wave, an upstroke being separated by a plateau phase from a downstroke. The main difference is, however, that the sine wave oscillator has a fixed frequency and its amplitude depends on its energy. The relaxation oscillator, on the other hand, has a variable frequency and a constant amplitude. This makes it an attractive candidate for modeling cardiac cells. In agreement with these characteristics, relaxation oscillators can be synchronized (which at one time made them very popular as timing elements in oscilloscope sweeps). Therefore, when coupled together, elements that have different intrinsic firing rates can synchronize each other and beat in unison, a thing the harmonic oscillator will not do. There is evidence that synchronization may play an important role in spontaneous rhythmicity, in the sinus node (van der Tweel et al., 1973), in cell cultures (Jongsma et al., 1975; Ypey et al., 1979), and in isolated Purkinje fibers (Jalife and Moe, 1976, 1979).

The trouble with van der Pol oscillators is that they cannot be stopped, and this makes them unsuitable for modeling nonautomatic cells. FitzHugh (1961) reformulated the van der Pol equations in terms of an autonomous system, and generalized the second equation, which describes the behavior of the excitability parameter (cf our Equation 1b), to an arbiratry straight line in the phase plane. The resulting formalism was similar to Bonhoeffer's famous nerve model (Bonhoeffer, 1948), in which a passive iron wire in nitric acid was used. For this reason, the new generalized van der Pol model was called the Bonhoeffer-van der Pol (BVP) model. The BVP model has a number of fascinating properties. It can be stimulated; there is a relative refractory period; repetitive activity can be turned on and off by polarizing currents. The time course of an activation can be described elegantly in electrophysiological terms. In addition, it is related both to the simple mathematical sine wave oscillator in the way just described and to the sophisticated Hodgkin-Huxley formulation of nerve activity. Indeed, it has been shown (FitzHugh, 1961) that it can be regarded as a close approximation of a two-dimensional projection of the four-dimensional (V, m, n, and h) Hodgkin-Huxley model.

For these reasons, we initially selected the BVP model for the present study. The results presented

in the section on focal tachycardias first were obtained from BVP elements (we did not try them in the circus movement tachycardias). Unfortunately, it has been difficult to obtain a satisfactory shape of the action potentials, since the repolarization phase, which tended to be too fast anyway, became very steep as soon as a plateau phase was introduced. Partially because of these cosmetic considerations and partially to have more liberty in the construction of excitable elements, we developed the present model.

The results presented above indicate that many of the characteristics of depressed myocardium can be simulated using very simple elements, if the interaction between the elements is taken into account. Electrotonic reflections of the activity of neighboring elements such as the "foot" in the trailing action potential and the hump in the plateau phase of the leading one (Fig. 5) often have been observed in experimental conditions, for instance in the AV node (Mendez and Moe, 1966), in Purkinje-muscle junctions (Mendez et al., 1969), in locally cooled Purkinje fibers (Downar and Waxman, 1976), and in coupled aggregates of embryonic heart cells (Ypey et al., 1979). They also have been evoked in extremely primitive (van Capelle and Janse, 1976), as well as more sophisticated, model studies (Lieberman et al., 1973).

More intriguing is the occurrence of subthreshold oscillations and the initiation and termination of focal repetitive activity by single stimuli. Similar phenomena have been described in Purkinje fibers exposed to digitalis and/or sodium-free solutions (Ferrier et al., 1973; Cranefield and Aronson, 1974) and in fibers of the simian mitral valve (Wit and Cranefield, 1976). We created the conditions for "triggered activity" (Wit and Cranefield, 1976) by a critical amount of coupling between pacemaker and nonpacemaker elements. This does not mean that the mechanism of triggered activity may not reside in altered cellular electrophysiological properties, irrespective of coupling. It has been shown theoretically (Cooley et al., 1965) that "hard" oscillations (that is, oscillatory activity in a system that also has a stable, nonoscillatory stationary state) may be found in Hodgkin-Huxley elements. Our results do show, however, that coupling of elements that lack this property themselves may easily result in this type of behavior, suggesting that the conditions for triggerable focal activity may be less restricted than commonly assumed. It is tempting, for instance, to speculate about the possible role of similar mechanisms during the occurrence of ischemic myocardial injury.

It is clear that spatial inhomogeneity in the instantaneous excitability of the elements is necessary for the establishment of one-way conduction and, therefore, for the initation of circus movement tachycardias. The present results do indicate however that the inhomogeneity may be conduction-induced and functional only, and that a dispersion of the intrinsic properties of the individual elements is not required (although it may help!). It is noteworthy, that in Moe's early model (1964) "fibrillation," i.e., sustained arrhythmias with multiple vortices, was evoked, which could be converted to CMT's (without an obstacle!) when the dispersion of refractory periods was abolished. In this model, which was governed by simple rules about refractoriness and conduction velocity, electrotonic interaction among the elements was not taken into account. It therefore appears that the occurrence of circus movement tachycardias in the homogenous sheet is not very sensitive to variations in the activation model used. Still, in our model, as well as in Gul'ko's, the inactivating influence of local depolarizing currents plays an important role, keeping the vortex partially inactivated so that it can behave functionally as an obstacle. This behavior is in agreement with experimental results on circus movement tachycardias in the rabbit left atrium (Allessie et al., 1977).

The size of a sheet was important for its susceptibility for CMT. In experimental CMT's in the rabbit atrium (Allessie et al., 1977) the diameter of the circuit was 6–8 mm. Assuming a value of 660 μm for the space constant of atrial tissue (Bonke, 1973), the circuit would comprise about 30 length constants. This agrees rather well with the critical size of our sheets which was about 20 length constants along the edges for the elements used. Comparison with the model of Moe et al. (1964) is more difficult, since electrotonic interaction was not accounted for in their model, and the size of their sheets therefore cannot be expressed in length constants. Still, since the minimum conduction velocity in their model was 0.25 unit/time step, and the refractory period of their elements ranged between 17 and 28 time steps, one can see that the smallest circuit theoretically possible in their model would consist of 4–7 elements. In our study, using the sheet depicted in Figure 10, the minimum conduction velocity was about 0.025 element/time step and the refractory period was about 800 time steps. Therefore, the lower bound for any circus movement was at least 20 elements in circumference. Our sheets therefore probably represent much smaller pieces of tissue than Moe's. The small size of our sheets explains why only rather depressed elements could be used to set up CMT's and why it was much more difficult in our case than in Moe's to evoke multiple vortices.

Comparing the characteristics of circus movement tachycardias in a homogenous sheet and in ring-like geometrics, we found that the tachycardias in the homogenous sheets were harder to start by stimulation but were also much harder to stop. Also, "resetting" of the phase of the tachycardia by stimulation was observed only in ring-like structures, where a relatively large part of the circuit is in an excitable state and can thus be interfered with by extraneous stimulation. The vortex of the tachycardias in the homogenous sheet, on the other

hand, seems to be well protected, which is in agreement with the considerations presented by Allessie on this problem (Allessie et al., 1977). Still, stimulation in the vicinity of the vortex did have an effect in our studies, since it resulted in an appreciable displacement of the site of the vortex. It remains to be seen whether this phenomenon would be likely to occur in actual heart tissue. The mobility of the vortex is natural enough in a homogenous medium, but heart tissue is inhomogeneous and anisotropic. It has been shown experimentally that, in left atrial preparations (Allessie et al., 1976), the locations at which circus movements could be evoked were related to local gradients in the duration of the refractory period. The site of the vortex is quite stable in such preparations, which makes it unlikely that free movement of the vortex plays an important role in experimental or clinical tachycardias, with the possible exception of fibrillation. Inhomogeneity of the preparation seems to make it easier to initiate this kind of tachycardia, because local block may occur so easily, but it also makes it easier to stop them, because the vortex is less likely to escape to another position in the preparation. The relevance of modeling this kind of tachycardia in homogeneous sheets lies mainly in the demonstration that dispersion in the intrinsic properties of the individual elements, however important its role, is definitely not necessary for this type of arrhythmia.

References

Allessie MA, Bonke FIM, Schopman FJG (1973) Circus movement in rabbit atrial muscle as a mechanism of tachycardia. Circ Res **33:** 54–62

Allessie MA, Bonke FIM, Schopman FJG (1976) Circus movement in rabbit atrial muscle as a mechanism of tachycardia II: The role of non uniform recovery of excitability in the occurrence of unidirectional block as studied with multiple microelectrodes. Circ Res **39:** 168–177

Allessie MA, Bonke FIM, Schopman FJG (1977) Circus movement in rabbit atrial muscle as a mechanism of tachycardia. III. The "leading circle" concept: A new model of circus movement in cardiac tissue without the involvement of an anatomical obstacle. Circ Res **41:** 9–18

Beeler GW, Reuter H (1977) Reconstruction of the action potential of ventricular myocardial fibres. J Physiol (Lond) **268:** 177–210

Bonhoeffer KF (1948) Activation of passive iron as a model for the excitation of nerve. J Gen Physiol **32:** 69–91

Bonke FIM (1973) Passive electrical properties of atrial fibers of the rabbit heart. Pfluegers Arch **339:** 1–15

Cooley JW, Dodge FA, Cohen H (1965) Digital computer solutions for excitable membrane models. J Cell Physiol **66:** 99–109

Cranefield PF, Aronson RS (1974) Initiation of sustained rhythmic activity by single propagated action potentials in canine cardiac Purkinje fibers exposed to sodium-free solutions or to ouabain. Circ Res **34:** 477–481

Downar E, Waxman MB (1976) Depressed conduction and unidirectional block in Purkinje fibers. *In* The Conduction System of the Heart, edited by HJJ Wellens, KI Lie, MJ Janse. Leiden, Stenfert Kroese, pp 393–409

Ferrier GR, Saunders JH, Mendez C (1973) A cellular mechanism for the generation of ventricular arrhythmias by acetylstrophanthidin. Circ Res **32:** 600–609

FitzHugh R (1961) Impulses and physiological states in theoretical models of nerve membrane. Biophys J **1:** 445–466

Gul'ko FB, Petrov AA (1972) Mechanism of the formation of closed pathways of conduction in excitable media. Biofizika **17:** 271–282

Jalife J, Moe GK (1976) Effect of electrotonic potentials on pacemaker activity of canine Purkinje fibers in relation to parasystole. Circ Res **39:** 801–808

Jalife J, Moe GK (1979) A biologic model of parasystole. Am J Cardiol **43:** 761–772

Jongsma HJ, Masson-Pevet M, Hollander CC, de Bruyne J (1975) Synchronization of beating frequency of cultured rat cells. *In* Developmental and Physiological Correlates of Cardiac Muscle, edited by M Lieberman, T Sano. New York, Raven Press, pp 185–196

Lieberman M, Kootsey JM, Johnson EA, Sawanobori T (1973) Slow conduction in cardiac muscle. A biophysical model. Biophys J **13:** 37–55

Mc Allister RE, Noble D, Tsien RW (1975) Reconstruction of the electrical activity of cardiac Purkinje fibres. J Physiol (Lond) **251:** 1–59

Mendez C, Moe GK (1966) Some characteristics of transmembrane potentials of AV nodal cells during propagation of premature beats. Circ Res **19:** 993–1010

Mendez C, Mueller WJ, Merideth J, Moe GK (1969) Interaction of transmembrane potentials in canine Purkinje fibers and at Purkinje fibre-muscle junctions. Circ Res **24:** 361–372

Mines GR (1914) On circulating excitations in heart muscles and their possible relation to tachycardia and fibrillation. Trans Roy Soc Canada (Biol) **8:** 43–52

Moe GK, Rheinboldt WC, Abildskov JA (1964) A computer model of atrial fibrillation. Am Heart J **67:** 200–220

Van Capelle FJL, Janse MJ (1976) Influence of geometry on the shape of the propagated action potential. *In* The Conduction System of the Heart, edited by HJJ Wellens, KI Lie, MJ Janse. Leiden, Stenfert Kroese, pp 316–335

Van der Pol B (1926) On relaxation oscillations. Phil Mag **2:** 978–992

Van der Pol B, van der Mark J (1928) The heartbeat considered as a relaxation oscillation and an electrical model of the heart. Philos Mag Suppl **6:** 763–775

Van der Tweel LH, Meijler FL, van Capelle FJL (1973) Synchronization of the heart. J Appl Physiol **34:** 283–287

Wit AL, Cranefield PF (1976) Triggered activity in cardiac muscle fibers of the simian mitral valve. Circ Res **38:** 85–98

Ypey DL, Clapham DE, DeHaan RL (1979) Development of electrical coupling and action potential synchrony between paired aggregates of embryonic heart cells. Membrane Biol **51:** 75–96